



Impacts of the heterogeneous ammonia uptake on air quality in the North China Plain

Yuxuan Lu^{1,3}, Ruonan Wang¹, Ningning Zhang¹, Qiyuan Wang¹, Yuepeng Pan², Qian Jiang¹, Xuexi Tie¹

5 ¹State Key Laboratory of Loess Science, Institute of Earth Environment, Chinese Academy of Sciences, Xi'an 710061, China

²State Key Laboratory of Atmospheric Boundary Layer Physics and Atmospheric Chemistry, Institute of Atmospheric Physics, Chinese Academy of Sciences, Beijing, 100029, China

³University of Chinese Academy of Sciences, Beijing 100049, China

10 *Correspondence to:* Ningning Zhang (zhangnn@ieecas.cn)

Abstract. Previous studies have revealed that the heterogeneous uptake of ammonia (NH₃) on secondary organic aerosols (SOA) profoundly influences the NH₃ budget, nitrate aerosol chemistry, and the regional PM_{2.5} burden, also constituting an important source of nitrogen-containing organic compounds (NOCs). However, current regional modeling efforts are hindered by large uncertainties in uptake coefficients (γ) and a persistent lack of field-based observational constraints. In this study, we incorporate a first-order reactive NH₃ uptake mechanism into the WRF-Chem model to evaluate its impacts on air quality and NOCs over the North China Plain (NCP) during November 2017, with a wide range of the uptake coefficient from 10⁻⁵ to 10⁻³. When simulations are constrained with available observations in the NCP, we conclude that the uptake coefficient of 10⁻⁵ is characterized as a conservative upper-bound estimate for this heterogeneous process. Sensitivity simulations with the uptake coefficient of 10⁻⁵ reveal that the uptake reaction decreases NH₃ concentrations by 0.62% and inorganic aerosol and PM_{2.5} concentrations by less than 0.06%, but contributes 1.2 $\mu\text{g m}^{-3}$ of NOCs in the NCP. This study suggests that the uptake reaction might be a vital path for NOCs formation, but its impact on air pollutants concentrations is insignificant.

15
20



1 Introduction

25 As the only primary alkaline gas in the atmosphere, ammonia plays an important role in the formation of atmospheric particulate matter, overall acidity of precipitation and atmospheric deposition of nitrogen to sensitive ecosystems (Behera et al., 2013; Cheng et al., 2016; Pye et al., 2020; Zheng et al., 2023). Major sources of NH_3 include animal waste, fertilizer application, combustion process and industrial emissions (Seinfeld & Pandis, 1998). In recent years, global ammonia emissions have shown a significant upward trend
30 (Clarisse et al., 2009; Liu et al., 2022; Xu et al., 2019; Ma et al., 2025). For instance, ammonia concentrations in Eastern Asia has increased by $75.7 \pm 6.3\%$, with an annually growth rate of $5.80 \pm 0.61\% \text{ yr}^{-1}$ (Van Damme et al., 2018). The NH_3 emissions in China, in particular, has been nearly tripled since 1980s due to rapid population growth (Fu et al., 2020). Both satellite and surface observations of NH_3 have confirmed that the North China Plain (NCP) is one of the largest NH_3 emission regions in the world (Van Damme et al., 2018). Moreover,
35 China's stringent emission control policies have substantially reduced acidic oxide concentrations since 2013, but inadvertently prolonged the atmospheric lifetime of NH_3 (Feng et al., 2021; Wu et al., 2017), contributing to frequent air pollution events in the NCP associated with high NH_3 levels (Wen et al., 2015; Fu et al., 2017; Lachatre et al., 2019).

Ammonia's chemical reactivity further underscores its significance in the atmosphere. It reacts with inorganic
40 acids (primarily sulfuric and nitric acids) to form low-volatility ammonium salts, which can easily condense into fine particulate matters. These acid-base reactions have been well-understood and incorporated into climate models (Luo et al., 2007; Makar et al., 2009). Meanwhile, gas-phase ammonia reacts with organic compounds in secondary organic aerosols (SOA) through two ways. It can either react with organic acids to form ammonium salts (Na et al., 2007) or participate in reactions with certain carbonyl compounds forming heterocyclic
45 nitrogen-containing organic compounds (NOCs).

The mechanism of ammonia uptake on SOA is first discovered in 2008 (Mang et al., 2008), and the formation of NOCs is confirmed later in laboratory experiments (Laskin et al., 2014; Nguyen et al., 2012). The generated NOCs contribute to atmospheric brown carbon (BrC), a type of light-absorbing organic aerosol with significant impacts on atmospheric chemistry, human health and climate forcing (Laskin et al., 2015; Moise et al., 2015).
50 Recent work has quantified NOCs as a constant component of fine particulate matters ($\text{PM}_{2.5}$) (1.4% on average), highlighting its potential role in regional radiative forcing (Wang et al., 2022b).

To evaluate the regional air quality implications of this NH_3 uptake process, several numerical modeling studies have been conducted using sensitivity experiments to bridge the gap between laboratory kinetics and



atmospheric scales. Zhu et al. (2018) have first incorporated this mechanism into a large-scale chemical
55 transport model (CTM) for the United States, testing a range of uptake coefficients (γ) from 10^{-5} to 10^{-3} and
considering 10^{-3} to be the upper limit γ . Their results have revealed that with the γ of 10^{-3} , domain-averaged
NH₃ concentrations are reduced by 31.3% in winter and up to 67.0% in summer. Notably, the study has also
demonstrated that the NH₃ uptake significantly promotes summer biogenic SOA production in the US through
enhanced acid-catalyzed pathways, with specific species like AISO₃ increasing by 16.2% even at a low γ
60 of 10^{-5} .

In the context of China's high-ammonia environment, Wu et al. (2021) have performed similar simulations
across mainland China. While their results have showed that the γ of 10^{-5} leads to only modest decreases in
average NH₃ mixing ratios (2.0% in summer and 4.8% in winter), the study have maintained 10^{-3} as the primary
upper-limit value for regional modeling. With the γ of 10^{-3} , they have predicted that the uptake reaction leads to
65 decreases in gas-phase NH₃ mixing ratios of 27.5% (summer) and 19.0% (winter). This depletion further
suppresses ammonium nitrate formation by as much as 30%, resulting in an overall PM_{2.5} reduction of
approximately 8.9% in summer and 8.7% in winter. Collectively, these studies underscore the profound
influence of NH₃-SOA interactions on regional atmospheric composition and PM budgets.

However, these previous studies predominantly rely on the γ of NH₃ uptake on SOA used in simulations, which
70 still has large uncertainties (Liu et al., 2015; Zhu et al., 2018; Wu et al., 2021). In addition, the absence of
simultaneous observations for both NH₃ and aerosol chemical components, particularly NOCs, causes
significant uncertainties in assessing the importance of this heterogeneous process in the regional atmospheric
environment. Therefore, it is imperative to evaluate impacts of the heterogeneous process on air quality
constrained by observations.

75 During November 2017, a field campaign in the NCP and its surroundings (NCPs) has been conducted, and an
extensive data set has been obtained, including observations of aerosol species, NH₃ and NOCs. In this study,
we first incorporate the heterogeneous uptake of NH₃ on SOA into the WRF-Chem. Constrained by the
available observations, one-month simulations are then performed to evaluate impacts of the uptake reaction on
the air quality in the NCP.

80

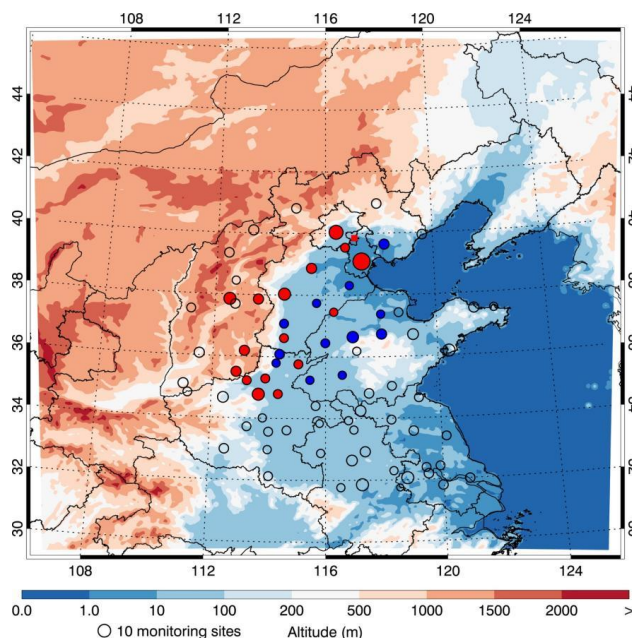
2 Model and Methodology

2.1 WRF-Chem model and measurements



A specific version of the WRF-Chem model is used in this study, modified by Li et al. (Li et al., 2010; Li et al., 2011a; Li et al., 2011b). The WRF-Chem simulations are conducted during November 2017 in the NCP. In the base simulation (hereafter referred to as BASE), the NH_3 uptake on SOA are not considered. Based on previous studies (e.g., Liu et al., 2015; Zhu et al., 2018; Wu et al., 2021), the γ of NH_3 on SOA is in the range between 10^{-5} and 10^{-3} . Therefore, three sensitivity simulations are devised, which are the same as the BASE but include the NH_3 uptake on SOA, with the γ of 10^{-3} , 10^{-4} and 10^{-5} , respectively (hereafter referred to as S(-3), S(-4), and S(-5)). Detailed information on the model description and configuration can be found in the Supplement (Text S1 and Table S1), and the simulation domain is presented in Fig. 1.

The WRF-Chem simulations in the BASE are validated using a comprehensive suite of observations, including hourly criteria pollutants ($\text{PM}_{2.5}$, O_3 , NO_2 , SO_2) from national networks and daily filter measured aerosol chemical components in the NCP. In-situ measurements of NH_3 and NOCs as well as IASI satellite products are also employed to verify model performances. Detailed descriptions are provided in S2 of the Supplement. The performance of the WRF-Chem model simulations is evaluated using metrics including the mean bias (*MB*), root mean square error (*RMSE*), and the index of agreement (*IOA*). Detailed description about *MB*, *RMSE*, and *IOA* can be found in S3 of the Supplement.



100 **Figure 1: WRF-Chem simulation domain with topography. The circles represent centers of cities with ambient monitoring sites, and the size of circles denotes the number of ambient monitoring sites of cities. The filled red circles denote those cities with continuous measurement of aerosol components, and the filled blue circles denote the cities with discontinuous measurements of aerosol components. The filled red rectangle indicates the Xianghe station.**



2.2 Parameterization of the NH₃ uptake

105 When a gas molecule strikes the surface of a particle, usually not every collision leads to reaction (Seinfeld & Pandis, 1998). Therefore, the γ is defined to express the probability of reactions and it is commonly determined by laboratory experiments. This study selects a plausible γ range of the NH₃ uptake on SOA ($\gamma = 10^{-3}$ ~ 10^{-5}) based on the laboratory results of Liu et al. (2015) and previous modeling studies (Wu et al., 2021; Zhu et al., 2018). The corresponding first-order reaction rate is then calculated using these coefficients and incorporated
110 into the model for sensitivity simulations. The first-order reaction rate of NH₃ uptake κ can be calculated as

$$\kappa = \gamma \times \frac{v_{\text{NH}_3} \times S_{\text{SOA}}}{4}, \quad (1)$$

Where γ is the uptake coefficient, v_{NH_3} is the mean speed of NH₃ molecules and S_{SOA} is the wet surface area concentration of SOA.

In this model, we assume that all heterogeneous reactions between NH₃ and SOA lead to the formation of NOCs,
115 which are subsequently removed by dry and wet deposition processes. In the real atmosphere, NH₃ can react with various SOA species to form NOCs. To simplify the simulation while retaining key chemical characteristics, SOA species are divided into three main categories based on their precursor origins: anthropogenic volatile organic compounds (VOCs), biogenic VOCs, and primary organic components. Each category is assigned a representative molecular weight, which is used in calculating NOCs concentrations. The
120 molecular weights for these SOA categories are adopted from a previously established model framework (Li et al., 2011).

3 Results and discussion

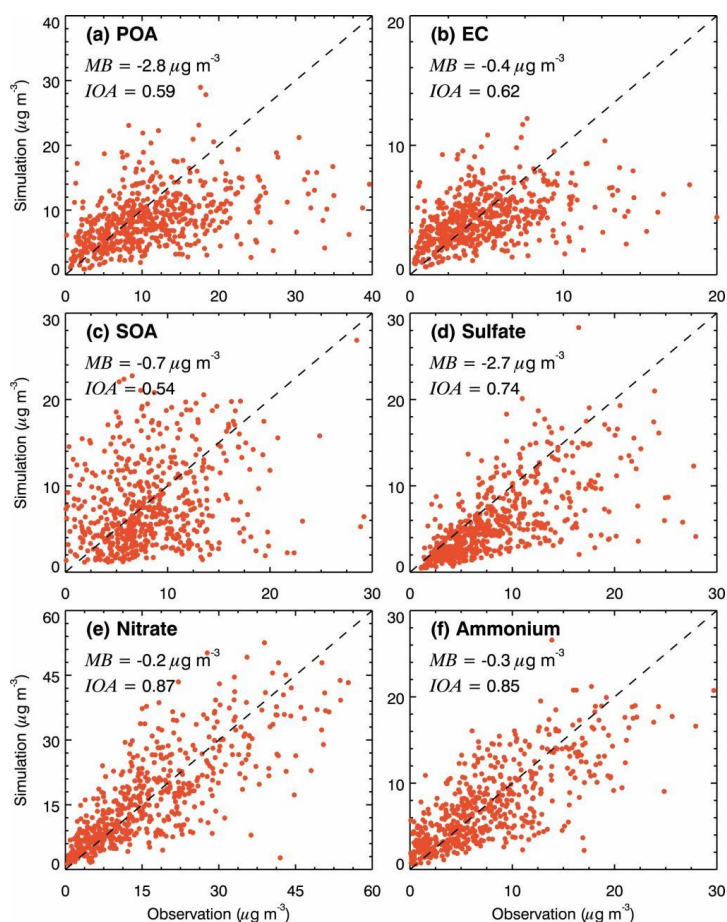
3.1 Model validation

125 Figure S2 presents the diurnal profiles of observed and simulated near-surface PM_{2.5}, O₃, NO₂, and SO₂ concentrations averaged at monitoring sites in the NCP during the simulation episode. The model well captures the temporal variations of these pollutants, with IOAs of 0.93, 0.84, 0.83 and 0.67, respectively. Figure S3 shows the simulated and observed spatial distributions of average mass concentrations of PM_{2.5}, O₃, NO₂, and SO₂ during the simulation episode. The simulated spatial patterns of these pollutants are in good agreement with
130 observations from ambient monitoring stations. Detailed model validation results are provided in S4 of the Supplement.

The simulated mass concentrations of key aerosol components are also evaluated against observations, including sulfate, nitrate, ammonia, elemental carbon (EC), primary organic aerosols (POA), and SOA (Fig. 2). The model



generally performs well in simulating the sulfate, nitrate and ammonium concentrations, with IOAs of 0.74, 0.87, and 0.85, respectively, but underestimates the sulfate concentration appreciably, with the MB of $-2.7 \mu\text{g m}^{-3}$. The model also reasonably reproduces POA, EC, and SOA concentrations, with the IOA of 0.59, 0.62, and 0.53, respectively. It is worth noting that the model tends to underestimate the carbonaceous aerosols, particularly with regarding to POA with a MB of $-2.8 \mu\text{g m}^{-3}$.



140 **Figure 2: Comparison of simulated and observed daily concentrations of (a) POA, (b) EC, (c) SOA, (d) sulfate, (e) nitrate and (f) ammonium aerosols at sites in NCP and its surrounding areas in November 2017.**

The simulated NH_3 vertical column densities (VCDs) show a generally good consistency with the IASI retrievals during the simulation period, with an IOA of 0.66 and MB of $0.26 \times 10^{16} \text{ molec cm}^{-2}$, indicating that the model generally reproduces the observed NH_3 VCDs with minimal systematic bias (Fig. 3a). Figure 3b displays the comparison of simulated and observed NH_3 concentrations at Xianghe station. The model demonstrates a good performance in simulating near-surface NH_3 concentrations, with the IOA of 0.66 and the



MB of -0.01 ppb. The monthly variation in NH_3 emissions is strongly influenced by agricultural practices and environmental conditions such as temperature and wind speed. During the simulation period, the observed NH_3 concentrations have exhibited several pronounced peak events in mid-November that the model fails to reproduce. These anomalies are likely associated with localized biomass burning activities (primarily crop and residential wood combustion), which are prevalent in the rural-urban fringe of the NCP during the transition to the heating season (Pan et al., 2018). These episodic emissions explain the discrepancy between simulations and observations.

Overall, the comprehensive validation against multi-source datasets indicates that the model exhibits a good performance in capturing the spatiotemporal variations of both criteria pollutants and NH_3 , providing a reliable foundation for the subsequent sensitivity analysis.

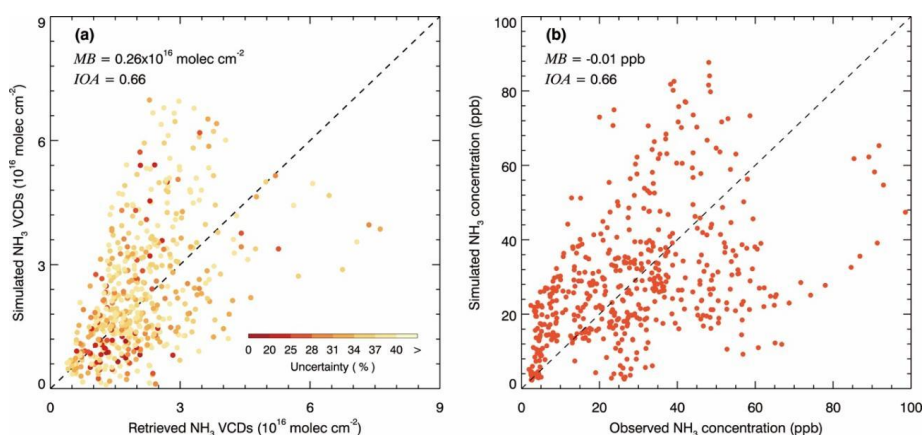


Figure 3: (a) Comparison between satellite retrieved and simulated NH_3 VCDs and (b) comparison of simulated and observed ammonia concentration at Xianghe in November 2017. In (a), the dot's color indicates the uncertainty (below 40%) of the retrieved NH_3 VCDs. In (a) and (b), the black dashed line represents the 1:1 reference line.

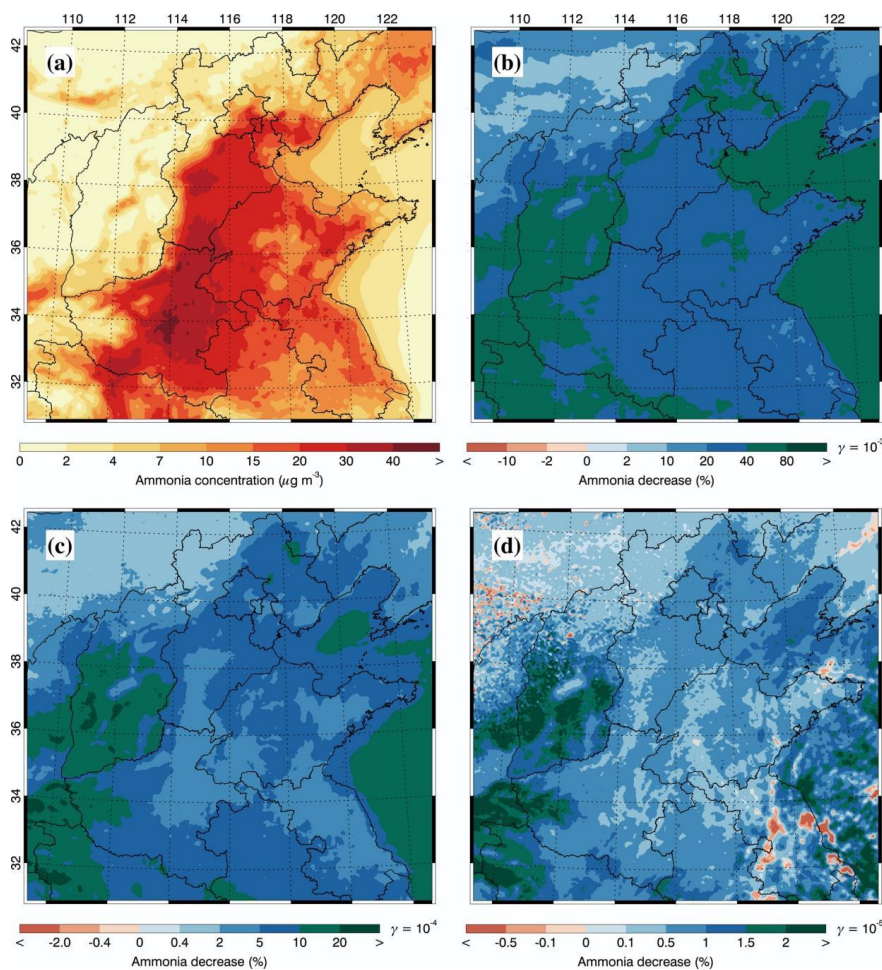
3.2 Impact of the uptake reaction on concentrations of NH_3 and aerosol components

Figure 4a shows the simulated distribution of average near-surface NH_3 concentrations during the simulation period. Quantitatively, the modeled NH_3 concentrations in the NCP range from 0.24 to 50.9 $\mu\text{g m}^{-3}$, with an average of 15.6 $\mu\text{g m}^{-3}$. These simulated NH_3 concentrations are within the range of observations reported in recent studies (Ianniello et al., 2010; Pan et al., 2018; Wang et al., 2022a; Zhang et al., 2021). For example, Ianniello et al. (2010) have reported that the observed daily average NH_3 concentrations in Beijing range from 0.20 to 44.38 $\mu\text{g m}^{-3}$, and Pan et al. (2018) have reported a regional annual average of 13.4 $\mu\text{g m}^{-3}$ over the NCP in 2015. Notably, the simulated NH_3 peak concentrations are concentrated in southern Hebei and eastern



Henan provinces, which has been further verified by recent emission constraints, showing sustained high nitrogen loading in these specific agricultural corridors (Liu et al., 2022; Yang et al., 2023).

Figures 4b-d illustrate the impacts of this uptake process on NH_3 concentrations in the S(-3), S(-4), and S(-5), by differentiating the S(-3), S(-4), and S(-5) with the BASE, respectively. In both S(-3) and S(-4), the uptake reaction reduces NH_3 concentration across the entire NCP. In the S(-3), the average decrease in the NCP is approximately 31.4% or $4.9 \mu\text{g m}^{-3}$, which is consistent with the findings of Wu et al. (2021), who have reported NH_3 reductions of 27.5% in summer and 19.0% in winter due to the NH_3 uptake on SOA. In the S(-4), the average NH_3 concentration decreases by 5.5% or $0.86 \mu\text{g m}^{-3}$, and the maximum reduction could reach 26.7%. For the S(-5), the NH_3 uptake reaction does not consistently decrease the NH_3 concentration in the NCP. The NH_3 concentration increases slightly in the southeast of the NCP. The average decrease of NH_3 concentrations is 0.62% or $0.096 \mu\text{g m}^{-3}$, with a maximum local reduction of 5.2%.

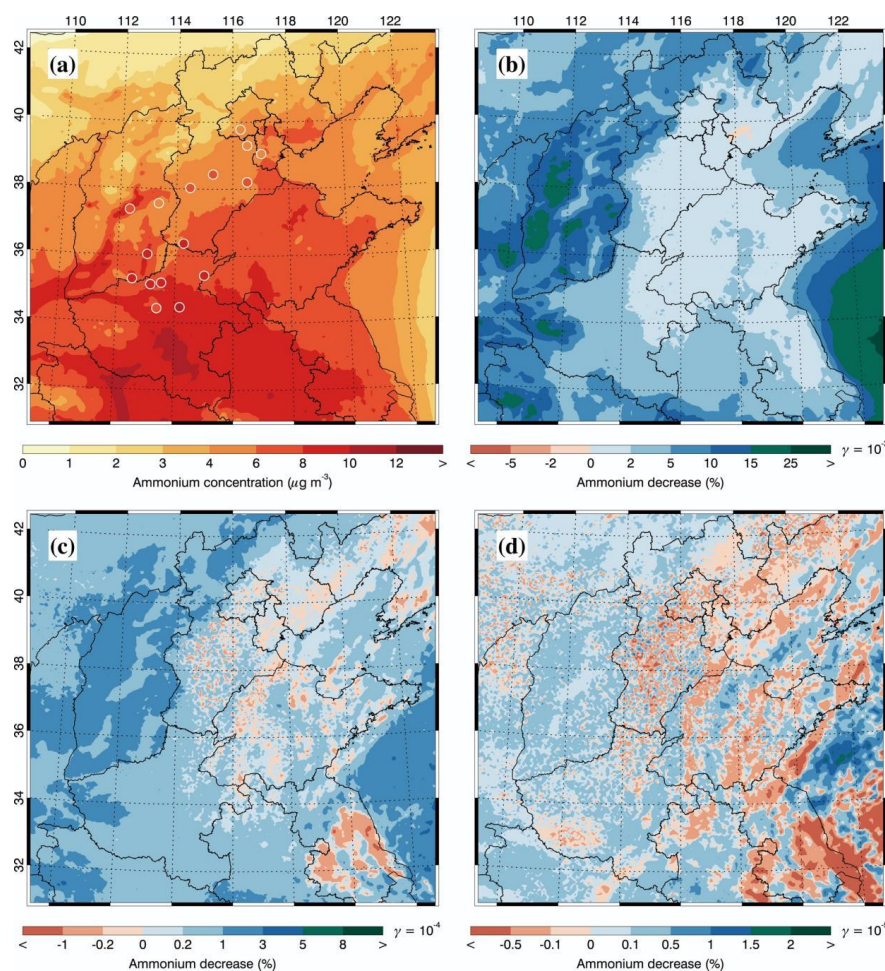




185 **Figure 4: (a) simulated (color contours) average near-surface mass concentrations of NH_3 and NH_3 concentration variation due to NH_3 uptake on SOA when the uptake coefficient equals (b) 10^{-3} , (c) 10^{-4} and (d) 10^{-5} in November 2017.**

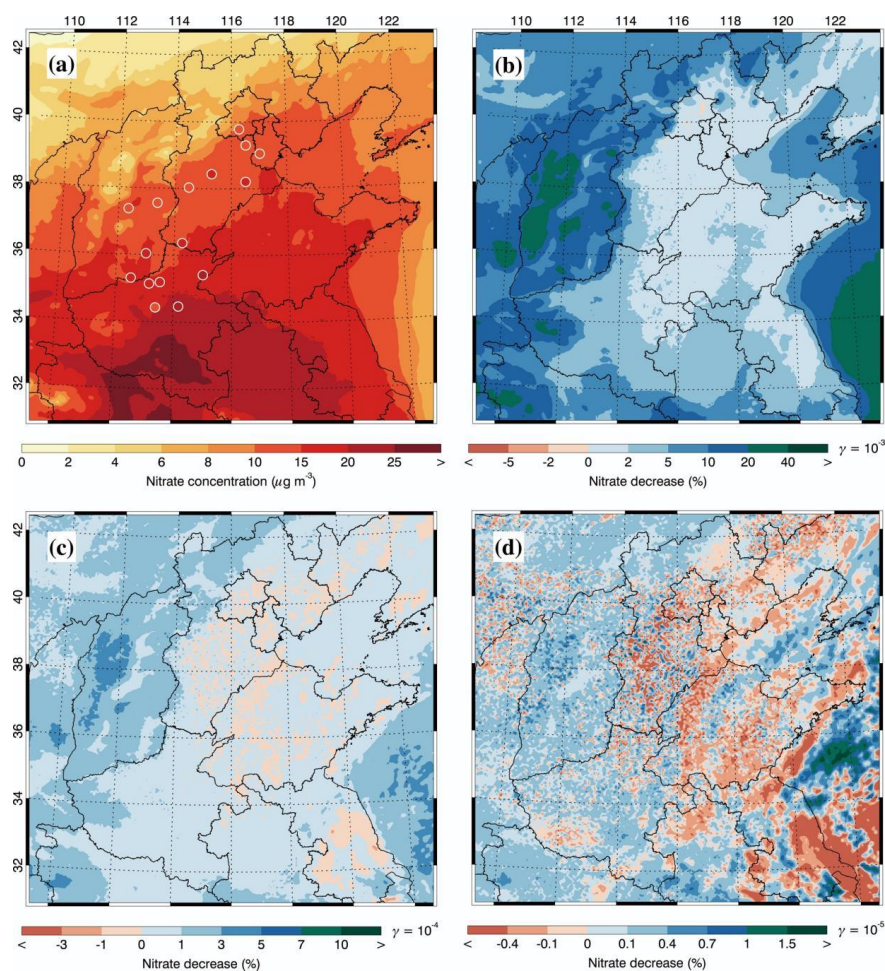
190 Considering that NH_3 serves as the sole precursor of ammonium aerosols, the perturbation of NH_3 concentrations due to its uptake on SOA directly influences the formation of ammonium aerosols in the atmosphere. Figure 5a shows the pattern comparison of average simulated and observed concentrations of ammonium aerosols during the simulated episode. Both the observation and simulation show the high ammonium concentrations in the south of the NCP, generally exceeding $8 \mu\text{g m}^{-3}$. In the S(-3), although the NH_3 uptake reaction decreases NH_3 concentrations by over 30% in the NCP, it only reduces the ammonium concentration by 5.5% or $0.86 \mu\text{g m}^{-3}$. The ammonium aerosol is formed by neutralizing sulfuric and nitric acids in the atmosphere. The observed and simulated high NH_3 level in the NCP indicates that NH_3 is excessive after
195 neutralizing inorganic acids to form ammonium salt. Hence, over a 30% decrease in NH_3 concentrations only causes a 5.5% reduction in ammonium aerosols in the NCP, a NH_3 -rich region. However, in the NH_3 -poor region, i.e., in Shanxi province and over oceans, ammonium concentrations decrease considerably.

200 Furthermore, the ammonium decrease in the NCP is not consistent, i.e., in the north of Beijing, the ammonium concentration increases slightly. Aerosols in the atmosphere directly scatter or absorb incoming solar radiation, inducing adjustments of the surface energy budget and the temperature profile, which further impact wind fields and transport of air species (IPCC, 2013). Apparently, the NH_3 uptake reaction has altered the aerosol concentrations, which perturbs wind fields to redistribute air species. Therefore, theoretically, the NH_3 uptake reaction should decrease ammonium concentrations consistently in the NCP, but the induced aerosol-radiation interactions (ARIs) change the ammonium distribution, causing an inconsistent variation of ammonium
205 concentrations. The increase in NH_3 concentrations due to the uptake reaction can also be observed in the S(-5). In the S(-4) and S(-5), the inconsistent variation of ammonium concentrations due to the uptake reaction becomes more significant. On average, the uptake reaction decreases the ammonium concentration slightly, with a decrease of 0.48% ($3.1 \times 10^{-2} \mu\text{g m}^{-3}$) and 0.048% ($3.1 \times 10^{-3} \mu\text{g m}^{-3}$) in the S(-3) and S(-4), respectively.



210 **Figure 5: (a) Pattern comparisons of simulated (color contours) versus observed (colored circles) average near-surface mass concentrations of ammonium aerosols and their variations due to NH_3 uptake on SOA when the uptake coefficient equals (b) 10^{-3} , (c) 10^{-4} and (d) 10^{-5} in November 2017.**

The decreased ammonium due to the uptake reaction potentially shifts the thermodynamic equilibrium
 215 of NH_4NO_3 toward the gas phase and leading to a decrease in particulate nitrate. The model generally well
 reproduces the nitrate distribution when comparing to observations (Fig. 6a). In the NCP, high nitrate
 concentrations are simulated, exceeding $10 \mu\text{g m}^{-3}$ and counting over 20% of $\text{PM}_{2.5}$ mass. In S(-3), the uptake
 reaction decreases nitrate concentrations by 4.6% ($0.70 \mu\text{g m}^{-3}$), and the decrease is generally consistent. In the
 S(-4) and S(-5), the decrease becomes inconsistent due to the induced ARIs, and is also insignificant. On
 220 average, the nitrate decrease is -0.56% ($8.5 \times 10^{-2} \mu\text{g m}^{-3}$) and -0.037% ($5.6 \times 10^{-3} \mu\text{g m}^{-3}$) in the S(-3) and S(-4),
 respectively.



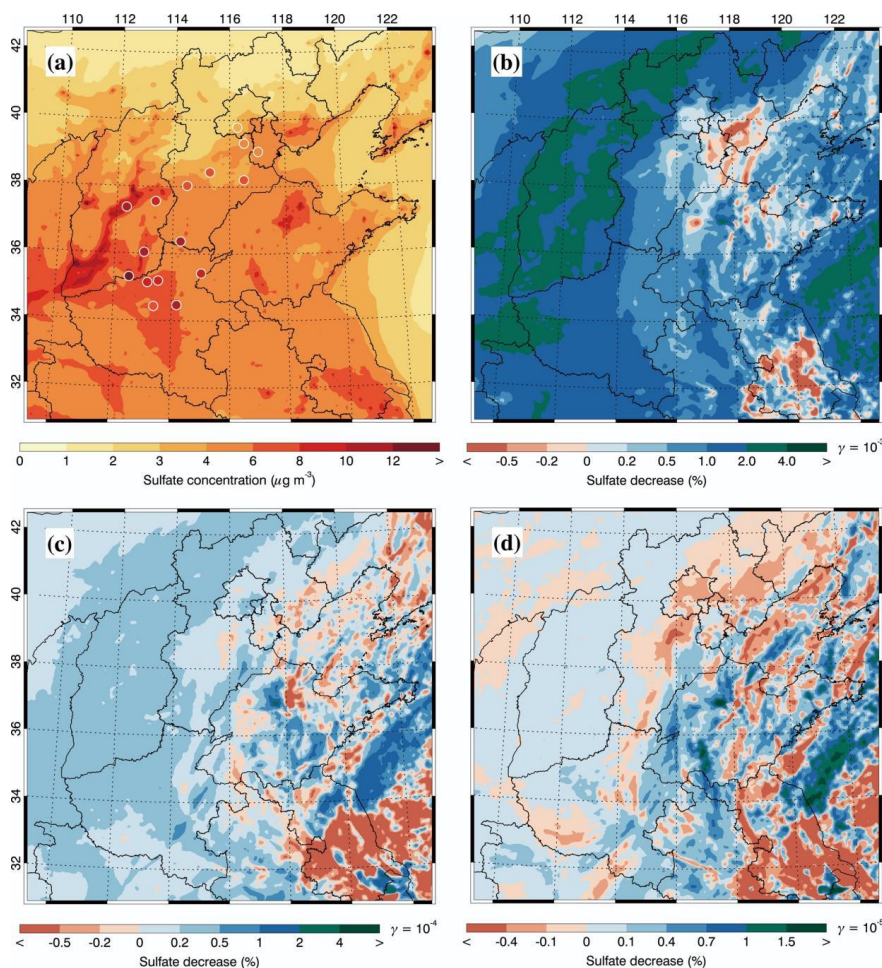
225 **Figure 6: (a) Pattern comparisons of simulated (color contours) versus observed (colored circles) average near-surface mass concentrations of nitrate aerosols and their variations due to NH_3 uptake on SOA when the uptake coefficient equals (b) 10^{-3} , (c) 10^{-4} and (d) 10^{-5} in November 2017.**

230 The reduction in available NH_3 can also lower the aerosol pH, thereby indirectly suppressing the aqueous-phase oxidation of SO_2 and potentially decreasing the formation rate of sulfate (Zhu et al., 2018; Zhang et al., 2020; Zhang et al., 2026). Considering the presence of excessive NH_3 in the NCP, the pH perturbation due to decreased NH_3 caused by the uptake reaction might not significantly impact sulfate formation. However, the SO_2 heterogeneous reaction involving aerosol liquid water (ALW) plays an important role in the sulfate formation (Li et al., 2017), so the decreased nitrate and ammonium aerosols due to the uptake reaction tend to reduce ALW content and hinder the sulfate formation. The simulated sulfate concentration in the NCP ranges from 3 to $10 \mu\text{g m}^{-3}$, and the model generally underestimates the sulfate concentration compared with observations (Fig. 7a). Since the decrease in ammonium and nitrate concentrations due to the uptake reaction is

235



not very significant, the resulting sulfate reduction is unimportant. On average, the sulfate decrease in the NCP is 1.1%, 0.16%, and 0.059% in the S(-3), S(-4), and S(-5), respectively. In addition, the sulfate variation becomes more and more inconsistent with decreasing uptake coefficient (Fig. 7b-d).

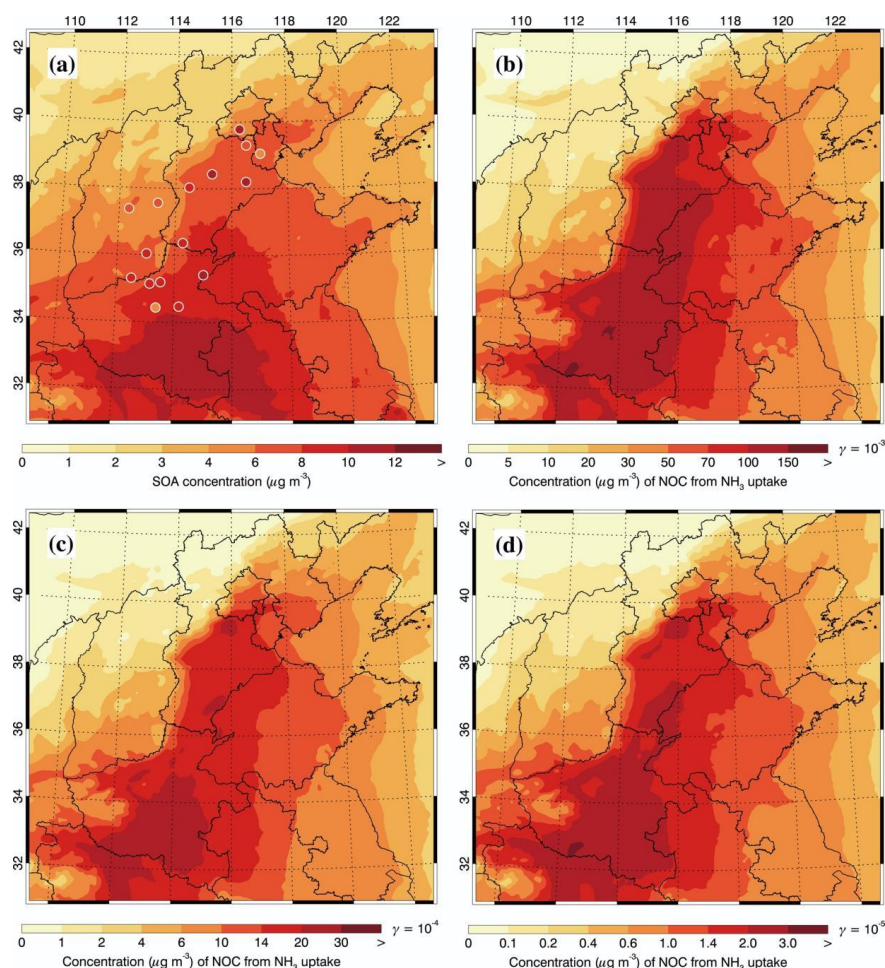


240 **Figure 7: (a) Pattern comparisons of simulated (color contours) versus observed (colored circles) average near-surface mass concentrations of sulfate aerosols and their variations due to NH₃ uptake on SOA when the uptake coefficient equals (b) 10⁻³, (c) 10⁻⁴ and (d) 10⁻⁵ in November 2017.**

In all the sensitivity simulations, all NH₃ uptake on SOA is assumed to produce NOCs but does not impact the
 245 SOA concentrations. The simulated SOA concentration in the NCP exceeds 6 µg m⁻³, with an average of 6.8 µg
 m⁻³ during the simulated episode. However, the model generally cannot well reproduce the observed high SOA
 concentrations in urban areas (Fig. 8a). The spatial pattern of particulate NOCs concentrations exhibits a clear
 consistency with that of NH₃ concentrations, and high NOCs concentrations are predominantly observed in
 regions with elevated NH₃ levels. Quantitative analysis of NOCs concentrations reveals remarkable



250 discrepancies between the high γ scenarios and real atmospheric conditions. In the S(-3), the model produces an unrealistically high NOCs burden, with the average concentration of $65.5 \mu\text{g m}^{-3}$, which is much far higher than the simulated SOA concentration (Fig. 4b). Similarly, although reducing the γ by an order of magnitude in the S(-4) markedly lowers the NOCs production, the average NOCs concentration of $11.3 \mu\text{g m}^{-3}$ remains much higher than the simulated SOA concentration. In contrast, the simulated average NOCs concentration in the S(-5) is $1.2 \mu\text{g m}^{-3}$, which is close to range of the observed NOCs concentrations. Wang et al. (2022b) have reported an average NOCs concentration of $1.27 \mu\text{g m}^{-3}$ at a regional site in Hebei, China. High levels of NOCs have been observed over the Tibetan region, with daily NOCs concentrations ranging from 0.71 to $3.89 \mu\text{g m}^{-3}$ and an average of $2.12 \pm 0.88 \mu\text{g m}^{-3}$ (Wang et al., 2024).



260 **Figure 8: (a) Pattern comparisons of simulated (color contours) versus observed (colored circles) near-surface mass concentrations of SOA and the near-surface NOCs concentration due to NH_3 uptake on SOA when the uptake coefficient equals (b) 10^{-3} , (c) 10^{-4} and (d) 10^{-5} in November 2017.**



Figure 9 shows the comparison of observed and simulated daily NOCs concentrations at Xianghe station in November 2017. The observed monthly average NOCs concentration is $1.52 \mu\text{g m}^{-3}$, ranging from 0.65 to $2.24 \mu\text{g m}^{-3}$. In the S(-3), the model simulates unrealistically high monthly average NOCs concentrations of $85.5 \mu\text{g m}^{-3}$ at the station. In the S(-4), the simulated concentration is $14.7 \mu\text{g m}^{-3}$, which remains far beyond the observation. Only in the S(-5) with the γ of 10^{-5} , the simulated concentration is $1.6 \mu\text{g m}^{-3}$, which is close to the observation. Therefore, although large γ values are expected to enhance NH_3 uptake and accelerate NOCs formation, the γ of 10^{-5} might be more reasonable to simulate the NH_3 uptake on SOA when the simulation is constrained by the observations of NH_3 and NOCs as well as other air species.

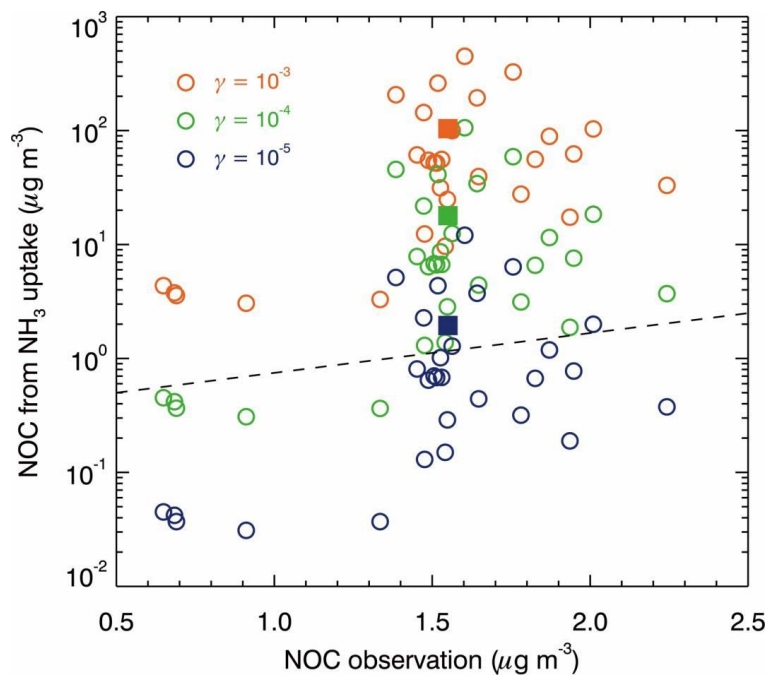


Figure 9: Comparison of observed and simulated near-surface daily NOCs concentrations at Xianghe station in November 2017.

275

Laboratory studies have suggested that the NH_3 uptake on SOA is limited, with only about 10% or less of SOA components reacting with NH_3 to form NOCs. This process is further characterized by a significant temporal decay in reaction efficiency, as demonstrated by Liu et al. (2015). In their experiments, initial γ values are on the order of 10^{-2} to 10^{-3} but drops to 10^{-5} in the later stages of the reaction. This reduction is primarily attributed to the continuous accumulation of organic aerosols on the particle surface, which acts as a physical barrier and increases particle viscosity. Such morphological changes induce a diffusion limitation that restricts NH_3 from

280



reaching the internal acid-catalyzed reaction sites, thereby suppressing the overall reactive uptake as the aerosol undergoes atmospheric aging.

In the real atmosphere, NOCs formation is also influenced by multiple processes. Except the uptake reaction examined here, a faster secondary pathway involves acid-base reactions between ammonia/ammonium and particulate organic acids (Laskin et al., 2009; Wang et al., 2017; Zhang et al., 2024). Primary emissions further contribute to NOCs levels, including emissions of biomass burning, coal combustion, vehicle emissions, biogenic production, and soil dust (Cheng et al., 2006; Harrison et al., 2005; Lu et al., 2019; Wang et al., 2022b).

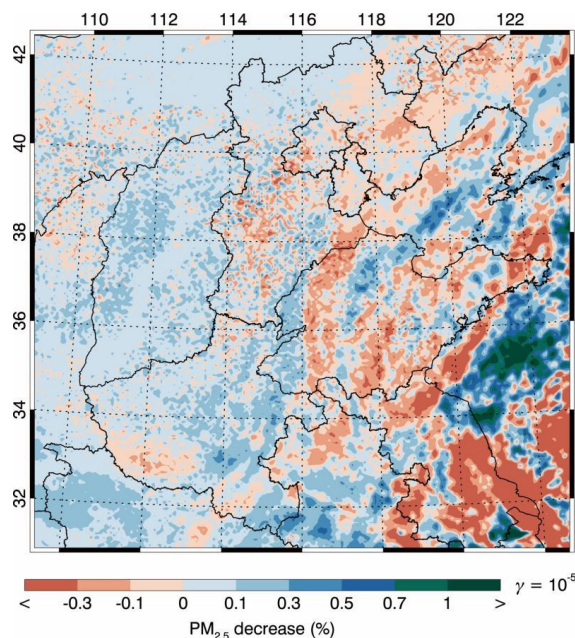
Given that NOCs concentrations simulated with the γ of 10^{-5} are the closest to observations and considering laboratory evidence of diminishing reaction activity over time, as well as the potential contribution from alternative pathways mentioned above, we conclude that the γ of 10^{-5} represents a reasonable upper limit for the γ in CTM simulations.

As discussed above, in the S(-5), impacts of the uptake reaction on inorganic salts is almost negligible in the NCP. This is partially attributed to NH_3 -rich conditions over the NCP, where only a very small fraction of NH_3 is consumed via the heterogeneous uptake on SOA, leaving most NH_3 available for reactions with inorganic acids and thereby limiting the influence of the process on inorganic aerosol formation. Consequently, $\text{PM}_{2.5}$ concentrations do not show substantial changes, with a slight decrease of 0.018% ($8.8 \times 10^{-3} \mu\text{g m}^{-3}$) in the NCP. The induced ARIs also cause an inconsistently variation of $\text{PM}_{2.5}$ concentrations (Fig. 10).

While previous studies have clearly demonstrated the potential importance of this heterogeneous uptake reaction (Zhu et al., 2018; Wu et al., 2021), the differences may arise from the diversity in chemical mechanisms across different models. Specifically, different models adopt distinct representations of gas-phase chemistry, heterogeneous reactions, and aerosol processes, which can lead to discrepancies in the production, transformation, and removal of atmospheric species. In addition, our simulations are constrained by observational evidence of both NH_3 and NOCs as well other air species, ensuring that the selected γ of 10^{-5} can be used to reasonably evaluate impacts of the uptake reactions on air quality. It is also worth noting that differences in simulation periods, seasonal conditions, and baseline chemical environments may further contribute to the discrepancies among studies. Under our simulation conditions with a high level of NH_3 and a small γ , the uptake reaction exerts a relatively small influence on NH_3 concentrations, and the corresponding perturbations to inorganic aerosols and $\text{PM}_{2.5}$ remain negligible. Under the high NH_3 condition in the study, the



PM_{2.5} variation due to the uptake reaction is also not substantial in the S(-3) and S(-4), with a decrease of 0.99% (2.0 μg m⁻³) and 0.26% (0.12 μg m⁻³), respectively.



315 **Figure 10: Average decrease of PM_{2.5} concentration due to the NH₃ uptake on SOA with the uptake coefficient of 10⁻⁵ in November 2017.**

4 Summary and conclusions

Recent studies have revealed that the heterogeneous uptake of NH₃ on SOA considerably influences the NH₃ budget, inorganic aerosol and PM_{2.5} concentrations, also constituting a critical pathway for NOCs formation. However, its magnitude remains uncertain due to poorly constrained uptake coefficients and limited field measurements of NOCs. In this study, we incorporated a first-order reactive NH₃ uptake mechanism into the WRF-Chem model and applied it to a severe PM_{2.5} pollution episode over the North China Plain (NCP) in November 2017. By varying the uptake coefficient from 10⁻⁵ to 10⁻³ based on values reported in previous laboratory and modeling studies and comparing the simulations with available observations, we evaluated the role of this heterogeneous process in regional air quality and NOCs formation.

The model generally well reproduced spatial distributions and temporal variations of PM_{2.5}, SO₂, NO₂, and O₃ concentrations when comparing to observations during the episode in the NCP. It also reasonably well simulates POA, EC, SOA, sulfate, nitrate, and ammonium against the measurement in the NCP. In addition, the model also performs reasonably in simulating the NH₃ concentration compared with satellite retrievals and in-situ



330 measurement at Xianghe station. The simulated mean NH_3 concentration over the NCP was $15.6 \mu\text{g m}^{-3}$,
indicating that the region was characterized by NH_3 -rich conditions during the episode.

Although the uptake reaction with a large uptake coefficient of 10^{-3} decreases the NH_3 concentration in the NCP
by over 30% and hinders formation of inorganic aerosols, it produces unrealistically high NOCs concentrations
of $65.5 \mu\text{g m}^{-3}$ averaged in the NCP during the episode. When the uptake coefficient is decreased to 10^{-4} , the
335 simulated NOCs concentration is $11.3 \mu\text{g m}^{-3}$, much higher than the simulated SOA concentration. Only when
the uptake coefficient is set to 10^{-5} , the simulated NOCs concentration is $1.2 \mu\text{g m}^{-3}$, in the range of observed
NOCs concentrations, and the simulated monthly NOCs concentration is comparable to the observations at
Xianghe station. Based on laboratory experiments and observational constraints, we conclude that the uptake
coefficient of 10^{-5} represents a reasonable upper limit for the NH_3 uptake reaction in CTM simulations.

340 Sensitivity simulations with the uptake coefficient of 10^{-5} reveal that the average decrease in NH_3 concentrations
is only 0.62% ($0.096 \mu\text{g m}^{-3}$) due to the uptake reaction. Furthermore, the uptake reaction exerts negligible
impacts on inorganic aerosol and $\text{PM}_{2.5}$ concentrations, and the induced decrease is less than 0.06%. The
negligible decrease might be partially due to the high background NH_3 levels in the NCP that limit the role of
this heterogeneous process. Overall, the influence of the uptake reaction on air pollutant concentrations is
345 insignificant in the NCP, but it might constitute an important source of NOCs.

It is worth noting that impacts of this uptake process are still subject to large uncertainties, due to the chemical
complexity of SOA, poorly constrained diffusivities of reactive species within SOA particles, and the scarcity of
field measurements of NOCs in polluted environments. Future work should combine more comprehensive field
measurements, laboratory constraints, and model development to better quantify the uptake coefficient and
350 evaluate the importance of this process across different atmospheric environments.

Taken together, this study provides an observation-constrained estimate of NH_3 uptake on SOA and clarifies its
atmospheric significance in a polluted, NH_3 -rich environment, improving our understanding of reduced nitrogen
partitioning and highlighting the need to better represent NOCs formation in chemical transport models.

355



Code and data availability

The hourly ambient surface O₃, NO₂, SO₂ and PM_{2.5} mass concentrations are real-timely released by Ministry of Ecology and Environment, China on the website <http://www.aqistudy.cn/>. The NH₃ total column products used
360 in this study were provided by the Infrared Atmospheric Sounding Interferometer (IASI) instruments on the Metop-B and Metop-C platforms, available through the IASI portal (<https://iasi.aeris-data.fr>).

Author contributions

NZ, as the corresponding author, provided the ideas, verified the conclusions, and revised the paper. YL
365 conducted research, designed the experiments, performed the simulation, processed the data, prepared the data visualization, and prepared the manuscript, with contributions from all authors. YP provided the primary data processing and reviewed the manuscript. RW and QJ analyzed the initial simulation data and visualized the model results. XT reviewed the manuscript and provided critical reviews.

370 Competing interests

The contact author has declared that none of the authors has any competing interests.

Disclaimer

Publisher's note: Copernicus Publications remains neutral with regard to jurisdictional claims made in the text,
375 published maps, institutional affiliations, or any other geographical representation in this paper. The authors bear the ultimate responsibility for providing appropriate place names. Views expressed in the text are those of the authors and do not necessarily reflect the views of the publisher.

Financial support

380 This research has been supported by the Key Research and Development Program of Shaanxi (grant 2024SF-ZDCYL-05-05) and the National Natural Science Foundation of China (grant 42307154).

References

385 Bauer, S. E., Balkanski, Y., Schulz, M., Hauglustaine, D. A., and Dentener, F.: Global modeling of heterogeneous chemistry on mineral aerosol surfaces: Influence on tropospheric ozone chemistry and comparison to observations, *J. Geophys. Res. Atmos.*, 109, D02304, <https://doi.org/10.1029/2003JD003868>, 2004.



-
- 390 Behera, S. N. and Sharma, M.: Transformation of atmospheric ammonia and acid gases into components of $PM_{2.5}$: an environmental chamber study, *Environ. Sci. Pollut. Res.*, 19, 1187–1197, <https://doi.org/10.1007/s11356-011-0635-9>, 2012.
- Behera, S., Sharma, M., Aneja, V., and Balasubramanian, R.: Ammonia in the atmosphere: A review on emission sources, atmospheric chemistry and deposition on terrestrial bodies, *Environ. Sci. Pollut. Res. Int.*, 20, 8092–8131, <https://doi.org/10.1007/s11356-013-2051-9>, 2013.
- 395 Bei, N., Li, G., and Molina, L. T.: Uncertainties in SOA simulations due to meteorological uncertainties in Mexico City during MILAGRO-2006 field campaign, *Atmos. Chem. Phys.*, 12, 11295–11308, <https://doi.org/10.5194/acp-12-11295-2012>, 2012.
- Bei, N., Wu, J., Feng, T., Bei, R., Zhao, S., Cao, J., Tie, X., and Li, G.: Impacts of Meteorological Uncertainties on the Haze Formation in Beijing-Tianjin-Hebei (BTH) during Wintertime: A case study, *Atmos. Chem. Phys.*, 17, 11679–11691, <https://doi.org/10.5194/acp-17-11679-2017>, 2017.
- 400 Binkowski, F. S. and Roselle, S. J.: Models-3 Community Multiscale Air Quality (CMAQ) model aerosol component 1. Model description, *J. Geophys. Res. Atmos.*, 108, 4183, <https://doi.org/10.1029/2001JD001409>, 2003.
- Chen, S., Cheng, M., Guo, Z., Xu, W., Du, X., and Li, Y.: Enhanced atmospheric ammonia (NH_3) pollution in China from 2008 to 2016: Evidence from a combination of observations and emissions, *Environ. Pollut.*, 263, 114421, <https://doi.org/10.1016/j.envpol.2020.114421>, 2020.
- Chen, X., Zhang, Y., Zhao, J., Zhou, W., Zhao, Y., and Li, G.: Regional modeling of secondary organic aerosol formation over eastern China: The impact of uptake coefficients of dicarbonyls and semivolatile process of primary organic aerosol, *Sci. Total Environ.*, 793, 148176, <https://doi.org/10.1016/j.scitotenv.2021.148176>, 2021.
- 410 Cheng, Y., Li, S.-M., and Leithead, A.: Chemical Characteristics and Origins of Nitrogen-Containing Organic Compounds in $PM_{2.5}$ Aerosols in the Lower Fraser Valley, *Environ. Sci. Technol.*, 40, 5846–5852, <https://doi.org/10.1021/es060385y>, 2006.
- Cheng, Y., Zheng, G., Wei, C., Mu, Q., Zheng, B., Wang, Z., Gao, M., Zhang, Q., He, K., Carmichael, G., Pöschl, U., and Su, H.: Reactive nitrogen chemistry in aerosol water as a source of sulfate during haze events in China, *Sci. Adv.*, 2, e1601530, <https://doi.org/10.1126/sciadv.1601530>, 2016.
- 415 Clarisse, L., Clerbaux, C., Dentener, F., Hurtmans, D., and Coheur, P.-F.: Global ammonia distribution derived from infrared satellite observations, *Nat. Geosci.*, 2, 479–483, <https://doi.org/10.1038/ngeo523>, 2009.
- Feng, T., Bei, N., Zhao, S., Wu, J., Kan, H., Tie, X., and Li, G.: Nitrate debuts as a dominant contributor to particulate pollution in Beijing: Roles of enhanced atmospheric oxidizing capacity and decreased sulfur dioxide emission, *Atmos. Environ.*, 244, 117995, <https://doi.org/10.1016/j.atmosenv.2020.117995>, 2021.
- 420 Fu, H., Luo, Z., and Hu, S.: A temporal-spatial analysis and future trends of ammonia emissions in China, *Sci. Total Environ.*, 731, 138897, <https://doi.org/10.1016/j.scitotenv.2020.138897>, 2020.
- Fu, X., Wang, S., Xing, J., Zhang, X., Wang, T., and Hao, J.: Increasing Ammonia Concentrations Reduce the Effectiveness of Particle Pollution Control Achieved via SO_2 and NO_x Emissions Reduction in East China, *Environ. Sci. Technol. Lett.*, 4, 221–227, <https://doi.org/10.1021/acs.estlett.7b00143>, 2017.
- 425 Harrison, M. A. J., Barra, S., Borghesi, D., Vione, D., Arsene, C., and Iulian Olariu, R.: Nitrated phenols in the atmosphere: a review, *Atmos. Environ.*, 39, 231–248, <https://doi.org/10.1016/j.atmosenv.2004.09.044>, 2005.



-
- Horne, J. R., Zhu, S., Montoya-Aguilera, J., Hinks, M. L., Wingen, L. M., Nizkorodov, S. A., and Dabdub, D.: Reactive uptake of ammonia by secondary organic aerosols: Implications for air quality, *Atmos. Environ.*, 189, 1–8, <https://doi.org/10.1016/j.atmosenv.2018.06.019>, 2018.
- 430 Ianniello, A., Spataro, F., Esposito, G., Allegrini, I., Hu, M., and Zhu, T.: Occurrence of gas phase ammonia in the area of Beijing (China), *Atmos. Chem. Phys.*, 10, 9487–9503, <https://doi.org/10.5194/acp-10-9487-2010>, 2010.
- Lachatre, M., Fortems-Cheiney, A., Foret, G., Siour, G., Dufour, G., Clarisse, L., Coheur, P.-F., Clerbaux, C., and Beekmann, M.: The unintended consequence of SO₂ and NO₂ regulations over China: increase of ammonia levels and impact on PM_{2.5} concentrations, *Atmos. Chem. Phys.*, 19, 6701–6716, <https://doi.org/10.5194/acp-19-6701-2019>, 2019.
- 435 Laskin, A., Desyaterik, Y., Alexander, M. L., Robinson, J. S., and Cowin, J. P.: Molecular characterization of nitrogen-containing organic compounds in biomass burning aerosols using high-resolution mass spectrometry, *Environ. Sci. Technol.*, 43, 3764–3771, <https://doi.org/10.1021/es803456n>, 2009.
- 440 Laskin, A., Laskin, J., and Nizkorodov, S. A.: Chemistry of Atmospheric Brown Carbon, *Chem. Rev.*, 115, 4335–4382, <https://doi.org/10.1021/cr5006167>, 2015.
- Laskin, J., Laskin, A., Nizkorodov, S., Roach, P., Eckert, P., Gilles, M. K., Wang, B., Lee, H. J., and Lin, P.: Molecular Selectivity of Brown Carbon Chromophores, *Environ. Sci. Technol.*, 48, 12047–12055, <https://doi.org/10.1021/es503038w>, 2014.
- 445 Li, G., Bei, N., Tie, X., and Molina, L. T.: Aerosol effects on the photochemistry in Mexico City during MCMA-2006/MILAGRO campaign, *Atmos. Chem. Phys.*, 11, 5169–5182, <https://doi.org/10.5194/acp-11-5169-2011>, 2011a.
- Li, G., Lei, W., Zavala, M., Volkamer, R., and Molina, L. T.: Impacts of HONO sources on the photochemistry in Mexico City during the MCMA-2006/MILAGO Campaign, *Atmos. Chem. Phys.*, 10, 6551–6567, <https://doi.org/10.5194/acp-10-6551-2010>, 2010.
- 450 Li, G., Zavala, M., Lei, W., Tsimpidi, A. P., Karydis, V. A., Pandis, S. N., Canagaratna, M. R., and Molina, L. T.: Simulations of organic aerosol concentrations in Mexico City using the WRF-CHEM model during the MCMA-2006/MILAGRO campaign, *Atmos. Chem. Phys.*, 11, 3789–3809, <https://doi.org/10.5194/acp-11-3789-2011>, 2011b.
- 455 Li, M., Su, H., Li, G., Ma, N., Pöschl, U., and Cheng, Y.: Relative importance of gas uptake on aerosol and ground surfaces characterized by equivalent uptake coefficients, *Atmos. Chem. Phys.*, 19, 10981–10111, <https://doi.org/10.5194/acp-19-10981-2019>, 2019.
- Liu, L., Xu, W., Lu, X., Zhong, B., Guo, Y., Liu, X., Sutton, M. A., Reis, S., and Galloway, J. N.: Exploring global changes in agricultural ammonia emissions and their contribution to nitrogen deposition since 1980, *Proc. Natl. Acad. Sci. U. S. A.*, 119, e2121998119, <https://doi.org/10.1073/pnas.2121998119>, 2022.
- 460 Liu, P., Li, Y. J., Wang, Y., Gilles, M. K., and Martin, S. T.: Highly Viscous States Affect the Browning of Atmospheric Organic Particulate Matter, *ACS Cent. Sci.*, 4, 207–215, <https://doi.org/10.1021/acscentsci.7b00452>, 2018.
- 465 Liu, P., Ding, J., and Liu, L.: Satellite Support to Estimate Livestock Ammonia Emissions: A Case Study in Hebei, China, *Atmosphere*, 13, 1644, <https://doi.org/10.3390/atmos13101644>, 2022.



- Liu, Y., Liggio, J., Staebler, R., and Li, S.-M.: Reactive uptake of ammonia to secondary organic aerosols: kinetics of organonitrogen formation, *Atmos. Chem. Phys.*, 15, 13569–13584, <https://doi.org/10.5194/acp-15-13569-2015>, 2015.
- 470 Lu, C., Wang, X., Li, R., Gu, R., Zhang, Y., Li, W., Gao, R., Chen, B., Xue, L., and Wang, W.: Emissions of fine particulate nitrated phenols from residential coal combustion in China, *Atmos. Environ.*, 203, 10–17, <https://doi.org/10.1016/j.atmosenv.2019.01.047>, 2019.
- Luo, C., Zender, C. S., Bian, H., and Metzger, S.: Role of ammonia chemistry and coarse mode aerosols in global climatological inorganic aerosol distributions, *Atmos. Environ.*, 41, 2510–2533, <https://doi.org/10.1016/j.atmosenv.2006.11.030>, 2007.
- 475 Ma, J., Shi, H., Zhu, Y., Li, R., Wang, S., Lu, N., Yao, Y., Bian, Z., and Huang, K.: The Evolution of Global Surface Ammonia Concentrations during 2001–2019: Magnitudes, Patterns, and Drivers, *Environ. Sci. Technol.*, 58, 2, 987–998, <https://doi.org/10.1021/acs.est.3c05193>, 2024.
- Makar, P. A., Moran, M. D., Zheng, Q., Cousineau, S., Sassi, M., Duhamel, A., Besner, M., Davignon, D., Crevier, L.-P., and Bouchet, V. S.: Modelling the impacts of ammonia emissions reductions on North American air quality, *Atmos. Chem. Phys.*, 9, 7183–7200, <https://doi.org/10.5194/acp-9-7183-2009>, 2009.
- 480 Mang, S. A., Henricksen, D. K., Bateman, A. P., Nizkorodov, S. A., and Laskin, J.: Contribution of Carbonyl Photochemistry to Aging of Atmospheric Secondary Organic Aerosol, *J. Phys. Chem. A*, 112, 8337–8344, <https://doi.org/10.1021/jp8043767>, 2008.
- 485 Moise, T., Flores, J. M., and Rudich, Y.: Optical Properties of Secondary Organic Aerosols and Their Changes by Chemical Processes, *Chem. Rev.*, 115, 4400–4439, <https://doi.org/10.1021/cr5005259>, 2015.
- Nguyen, T. B., Laskin, J., Laskin, A., and Nizkorodov, S. A.: Formation of nitrogen- and sulfur-containing light-absorbing compounds accelerated by evaporation of water from secondary organic aerosols, *J. Geophys. Res. Atmos.*, 117, D01207, <https://doi.org/10.1029/2011JD016944>, 2012.
- 490 Pan, Y., Tian, S., Zhao, Y., Zhang, L., Zhu, B., Gao, J., Huang, J., Chang, Y., Zhu, Y., He, H., Zhang, H., Zhang, L., Wu, Q., Zheng, H., Song, K., Zhou, F., Tian, B., Pan, Z., Huang, S., Wu, J., Liu, Y., Xu, W., Cheng, L., Liu, X., and Wang, Z.: Identifying Ammonia Hotspots in China Using a National Observation Network, *Environ. Sci. Technol.*, 52, 3926–3934, <https://doi.org/10.1021/acs.est.7b05235>, 2018.
- 495 Pye, H. O. T., Nenes, A., Alexander, B., Ault, A. P., Barth, M. C., Clegg, S. L., Collett Jr., J. L., Fahey, K. M., Hennigan, C. J., Herrmann, H., Kanakidou, M., Kelly, J. T., Ku, I. T., McNeill, V. F., Riemer, N., Schaefer, T., Shi, G., Tilgner, A., Walker, J. T., Wang, T., Weber, R., Xing, J., Zaveri, R. A., and Zuend, A.: The acidity of atmospheric particles and clouds, *Atmos. Chem. Phys.*, 20, 4809–4888, <https://doi.org/10.5194/acp-20-4809-2020>, 2020.
- Seinfeld, J. H. and Pandis, S. N.: *Atmospheric chemistry and physics: from air pollution to climate change*, John Wiley & Sons, New York, 1326 pp., 1998.
- 500 Tie, X., Madronich, S., Walters, S., Edwards, D. P., Ginoux, P., Rasch, P., Zhang, R., and Brasseur, G.: Effect of clouds on photolysis and oxidants in the troposphere, *J. Geophys. Res. Atmos.*, 108, 4642, <https://doi.org/10.1029/2003JD003659>, 2003.
- Updyke, K. M., Nguyen, T. B., and Nizkorodov, S. A.: Formation of brown carbon via reactions of ammonia with secondary organic aerosols from biogenic and anthropogenic precursors, *Atmos. Environ.*, 63, 22–31, <https://doi.org/10.1016/j.atmosenv.2012.09.012>, 2012.



-
- Van Damme, M., Clarisse, L., Whitburn, S., Hadji-Lazaro, J., Hurtmans, D., Clerbaux, C., and Coheur, P.-F.: Industrial and agricultural ammonia point sources exposed, *Nature*, 564, 99–103, <https://doi.org/10.1038/s41586-018-0747-1>, 2018.
- 510 Wahner, A., Mentel, T. F., Sohn, M., and Stier, J.: Heterogeneous reaction of N_2O_5 on sodium nitrate aerosol, *J. Geophys. Res. Atmos.*, 103, 31103–31112, <https://doi.org/10.1029/98JD02203>, 1998.
- Wang, X. F., Wang, H. L., Jing, H., Wang, W. N., Cui, W. D., and Williams, B. J.: Formation of nitrogen-containing organic aerosol during combustion of high-sulfur-content coal, *Energy Fuels*, 31, 14161–14168, <https://doi.org/10.1021/acs.energyfuels.7b02570>, 2017.
- 515 Wang, C., Li, X., Zhang, T., A., Cui, M., Liu, X., Ma, X., Zhang, Y., Liu, X., and Zheng, M.: Developing Nitrogen Isotopic Source Profiles of Atmospheric Ammonia for Source Apportionment of Ammonia in Urban Beijing, *Front. Environ. Sci.*, 10, 854340, <https://doi.org/10.3389/fenvs.2022.903013>, 2022 (a).
- Wang, M., Wang, Q., Ho, S. S. H., Li, H., Zhang, R., Ran, W., Qu, L., Lee, S. C., and Cao, J.: Chemical characteristics and sources of nitrogen-containing organic compounds at a regional site in the North China Plain during the transition period of autumn and winter, *Sci. Total Environ.*, 812, 151451, <https://doi.org/10.1016/j.scitotenv.2021.151451>, 2022 (b).
- Wang, M., Wang, Q., Ho, S. S. H., Tian, J., Zhang, Y., Lee, S., and Cao, J.: Dominant influence of biomass combustion and cross-border transport on nitrogen-containing organic compound levels in the southeastern Tibetan Plateau, *Atmos. Chem. Phys.*, 24, 11175–11189, <https://doi.org/10.5194/acp-24-11175-2024>, 2024.
- 525 Wen, L., Chen, J., Yang, L., Wang, X., Peng, C., Sui, R., Yao, L., and Li, Y.: Enhanced formation of fine particulate nitrate at a rural site on the North China Plain in summer: The important roles of ammonia and ozone, *Atmos. Environ.*, 101, 294–302, <https://doi.org/10.1016/j.atmosenv.2014.11.037>, 2015.
- Wesely, M. L.: Parameterization of surface resistances to gaseous dry deposition in regional-scale numerical models, *Atmos. Environ.*, 23, 1293–1304, [https://doi.org/10.1016/0004-6981\(89\)90153-4](https://doi.org/10.1016/0004-6981(89)90153-4), 1989.
- 530 Whitby, E. R. and McMurry, P. H.: Modal Aerosol Dynamics Modeling, *Aerosol Sci. Technol.*, 27, 673–688, <https://doi.org/10.1080/02786829708965508>, 1997.
- Whitburn, S., Van Damme, M., Clarisse, L., Bauduin, S., Heald, C. L., Hadji-Lazaro, J., Clerbaux, C., and Coheur, P.-F.: A flexible and robust neural network IASI- NH_3 retrieval algorithm, *J. Geophys. Res.-Atmos.*, 121, 6581–6599, <https://doi.org/10.1002/2016JD024828>, 2016.
- 535 Wu, J., Li, G., Cao, J., Bei, N., Wang, Y., Feng, T., Huang, R.-J., Liu, S., Zhang, Q., and Tie, X.: Contributions of trans-boundary transport to summertime air quality in Beijing, China, *Atmos. Chem. Phys.*, 17, 2035–2051, <https://doi.org/10.5194/acp-17-2035-2017>, 2017.
- Wu, K., Zhu, S., Liu, Y., Zhang, J., and Li, G.: Modeling Ammonia and Its Uptake by Secondary Organic Aerosol Over China, *J. Geophys. Res.-Atmos.*, 126, e2020JD034109, <https://doi.org/10.1029/2020JD034109>, 2021.
- 540 Xu, R., Tian, H., Pan, S., Prior, S. A., Feng, Y., Batchelor, W. D., Chen, J., and Yang, J.: Global ammonia emissions from synthetic nitrogen fertilizer applications in agricultural systems: Empirical and process-based estimates and uncertainty, *Glob. Change Biol.*, 25, 314–326, <https://doi.org/10.1111/gcb.14498>, 2019.
- Yang, S. L., Wang, M. Y., and Wang, M. S.: Establishing an emission inventory for ammonia, a key driver of haze formation in the southern North China plain during the COVID-19 pandemic, *Sci. Total Environ.*, 904, 171545, <https://doi.org/10.1016/j.scitotenv.2023.171545>, 2023.



-
- Zhang, G., Lian, X., Fu, Y., Lin, Q., Li, L., Song, W., Wang, Z., Tang, M., Chen, D., Bi, X., Wang, X., and Sheng, G.: High secondary formation of nitrogen-containing organics (NOCs) and its possible link to oxidized organics and ammonium, *Atmos. Chem. Phys.*, 20, 1469–1481, <https://doi.org/10.5194/acp-20-1469-2020>, 2020.
- 550 Zhang, R., Han, Y., Shi, A., et al.: Characteristics of ambient ammonia and its effects on particulate ammonium in winter of urban Beijing, China, *Environ. Sci. Pollut. Res.*, 28, 62828–62838, <https://doi.org/10.1007/s11356-021-15127-z>, 2021.
- Zhang, G., Wang, T., Lin, Q., Liu, K., Sun, W., Chen, D., Li, L., Wang, X., and Bi, X.: A comparative study on the formation of nitrogen-containing organic compounds in cloud droplets and aerosol particles, *J. Environ. Sci.*, 146, 266–275, <https://doi.org/10.1016/j.jes.2024.01.026>, 2024.
- 555 Zhang, G., Li, T., Sun, W., Huang, X., Wang, T., Wang, X., Ma, N., Hu, W., Tang, M., Shi, Z., Wang, X., Peng, P., and Bi, X.: Molecular Evidence of Aqueous-Processed NOCs: From Mechanistic Insights to Environmental Impacts, *J. Geophys. Res. Atmos.*, 131, e2025JD045757, <https://doi.org/10.1029/2025JD045757>, 2026.
- 560 Zheng, G., Su, H., and Cheng, Y.: Role of Carbon Dioxide, Ammonia, and Organic Acids in Buffering Atmospheric Acidity: The Distinct Contribution in Clouds and Aerosols, *ACS Earth Space Chem.*, 7, 1845–1856, <https://doi.org/10.1021/acsearthspacechem.3c00125>, 2023.
- Zhu, S., Horne, J. R., Montoya-Aguilera, J., Zhu, L., Wang, L., and Chen, X.: Modeling reactive ammonia uptake by secondary organic aerosol in CMAQ: application to the continental US, *Atmos. Chem. Phys.*, 18, 3641–3657, <https://doi.org/10.5194/acp-18-3641-2018>, 2018.
- 565 Zhu, S., Wu, K., Nizkorodov, S. A., and Dabdub, D.: Modeling reactive ammonia uptake by secondary organic aerosol in a changing climate: a WRF-CMAQ evaluation, *Front. Environ. Sci.*, 10, 867908, <https://doi.org/10.3389/fenvs.2022.867908>, 2022.